JOURNAL OF GEOPHYSICAL RESEARCH, VOL. 112, D24105, doi:10.1029/2007JD008744, 2007

Role of moist energy advection in formulating anomalous Walker Circulation associated with El Niño

Yoo-Geun Ham,[1] Jong-Seong Kug,[2] and In-Sik Kang[1,3]

Received 2 April 2007; revised 3 August 2007; accepted 22 August 2007; published 25 December 2007.

[1] The role of meridional moist energy advection in formulating anomalous Walker Circulation during El Niño events is investigated using observational data and linearized GCM. During the El Niño mature phase, the warm pool is extended to the central Pacific, so that the magnitudes of equatorial SST become uniform over the western-central Pacific. In contrast to the uniform SST distribution over the western-central Pacific, the maximum of equatorial convective activities are zonally displaced from the western to the central Pacific. That is in line with the fact that the strong anomalous descending motions are located over the western Pacific without local negative SST anomalies. It is demonstrated here that suppressed convection over the western Pacific is associated with cold-dry moist energy advection due to low-level equatorward winds. The meridional cold-dry moist energy advection leads the vertical warm-wet moist energy advection and adiabatic warming processes (descending motion) to balance the moist energy budget. It is shown that this meridional wind is a part of a cyclonic Rossby wave in response to the anomalous convection induced by El Niño SST. This mechanism, suggested here, is validated by using a linearized GCM. The model results show the downward branch of the anomalous Walker Circulation over the western Pacific is significantly reduced when the moist energy advection is not allowed.

Citation: Ham, Y.-G., J.-S. Kug, and I.-S. Kang (2007), Role of moist energy advection in formulating anomalous Walker Circulation associated with El Niño, *J. Geophys. Res.*, *112*, D24105, doi:10.1029/2007JD008744.

1. Introduction

[2] Zonal displacement of the convection center from the western to the central Pacific is one of the most prominent changes associated with El Niño [*Kidson*, 1975; *Saravanan and Chang*, 2000]. The anomalous Walker Circulation pattern, which results from zonal displacement in convection during El Niño, has also been investigated by many researchers [*Lau and Nath*, 2003; *Watanabe and Jin*, 2003; *Su and Neelin*, 2002; *Chou*, 2004; *Wang*, 2000; *Wu and Wang*, 2000; *Kang et al.*, 2002; *Kug and Kang*, 2006; *Annamalai et al.*, 2007]. There is general agreement that positive precipitation anomalies over the central Pacific can be attributed to positive sea surface temperature anomalies over the central and eastern Pacific. However, the mechanisms associated with the anomalous descent over the western Pacific are not clearly understood.

[3] One of the main reasons for inducing the anomalous descent is to compensate for the upward motions over the central Pacific associated with El Niño. *Lau and Nath* [2003] mentioned that the warm SST anomalies over the eastern Pacific weaken the downward branch of the Walker Circulation, which might induce anomalous subsidence over the western Pacific. However, they did not provide a detailed mechanism of how subsidence over the western Pacific might be induced by warm SST anomalies over the eastern Pacific.

[4] In fact, there is still controversy whether positive SST anomalies over the eastern Pacific can generate a descent over the western Pacific near the equator. For example, *Chou* [2004] claimed that simulated precipitation anomalies over the western Pacific are significant when only the eastern Pacific SST anomalies are prescribed. However, *Su and Neelin* [2002] showed that their own model failed to simulate the downward anomalies over the western Pacific when the SST anomalies over the eastern Pacific are prescribed. They argued that the missing downward anomalies in the western Pacific are mostly contributed by local SST anomalies. Similar to Su and Neelin's suggestion, *Wang* [2000] showed that the local SST anomalies are important in modulating atmospheric circulation over the western Pacific using their simple model.

[5] As well as warm SST anomalies over the eastern Pacific and the local SST anomalies over the western Pacific, some previous studies have argued that the warm SST anomalies over the Indian Ocean play an important role on modulating Walker Circulation during El Niño [*Watanabe and Jin*, 2003; *Annamalai et al.*, 2005b; *Kug and Kang*, 2006; *Kug et al.*, 2006a, 2006b]. For example, *Annamalai et al.* [2005b] argued that more than 50% of the total

[1]School of Earth and Environment Sciences, Seoul National University, Seoul, South Korea.
[2]Climate Environment System Research Center, Seoul National University, Seoul, South Korea.
[3]Also at Climate Environment System Research Center, Seoul National University, Seoul, South Korea.

0148-0227/07/2007JD008744$09.00

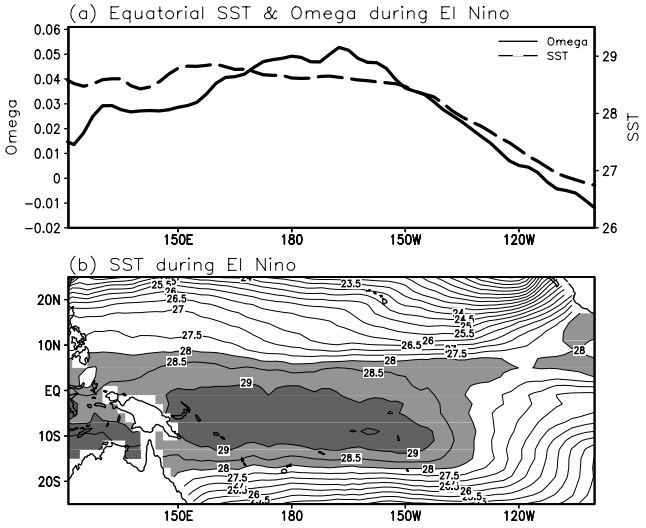

Figure 1. (a) Equatorial (10°S–10°N) vertical pressure velocity at 500 hPa and SST and (b) spatial distribution of SST during the five largest El Niño events. The sign of vertical pressure velocity is reversed.

precipitation anomalies over the tropical west Pacific-Maritime Continent are forced by remote Indian Ocean SST anomalies.

[6] On the other hand, *Kang et al.* [2002] demonstrated that most GCMs failed to simulate precipitation anomalies over the western Pacific for the 1997/1998 El Niño, even when observed SST anomalies associated with El Niño are prescribed. They also concluded that neither positive SST anomalies over the eastern Pacific and Indian Ocean nor local negative SST anomalies are sufficient for the suppressed convection over the western Pacific.

[7] Though many mechanisms are proposed and discussed as mentioned before, the mechanism related to the zonal displacement of the convection center during El Niño is still a controversial issue; therefore it is worthwhile to investigating how the Walker Circulation is changed associated with El Niño. During the El Niño, equatorial SST from western to central Pacific becomes uniform as SST anomalies over the western Pacific (central Pacific) are slightly lower (higher) than normal. It is interesting that, although equatorial SST is uniform from the western to central Pacific, the convective activities are at a maximum over the central Pacific during El Niño. Figure 1 shows the 500 hPa vertical pressure velocities and SST field during the mature phase (DJF) of 5 largest El Niño. During the El Niño events, the convective activities are maxima over the central Pacific though the magnitude of equatorial SST from the western to central Pacific is nearly uniform. This means that the magnitude of upward motion is not simply a maximum over the region where high SST is. This implies that another dynamical process, as well as the effect of SST, plays a role in modulating the Walker Circulation during El Niño. In this study, we investigate the dynamics associated with the modulation of the Walker Circulation and suggest that meridional advection of moist energy is responsible for the zonal displacement of convection during the El Niño mature phase.

[8] Section 2 introduces the observation data and model utilized. In section 3, we demonstrate the role of moist energy advection on the zonal displacement of the convection center during the El Niño mature phase using observed data. How linearized atmospheric GCM experiments support our hypothesis is discussed in section 4. The summary and discussion are given in section 5.

2. Data and Model

[9] The data utilized are monthly means of sea surface temperature (SST), atmospheric circulation data. The SST data were obtained from the National Centers for Environmental Prediction (NCEP), and were constructed on the basis of the EOF of observed SST [*Reynolds*, 1988] and reconstructed after January 1981 using the optimum interpolation technique [*Reynolds and Smith*, 1994]. Atmospheric circulation data were taken from National Centers for Environmental Prediction/ National Center for Atmospheric Research (NCEP/NCAR [*Kalnay et al.*, 1996]). They have a horizontal resolution of 2.5° × 2.5°. The period from which the data is taken is the 43 years from 1958 to 2000.

[10] As well as the atmospheric variables, monthly mean CMAP precipitation data, whose horizontal resolution is 2.5° × 2.5°, is also used from 1979 to 2000 [*Xie and Arkin*, 1997]. Other precipitation data used in this study correspond to retrievals from Tropical Rainfall Measuring Mission (TRMM) satellite Microwave Imager (TMI) measurements. The TRMM data set corresponds to monthly averaged precipitation with a spatial resolution of 0.25° from 40°S–40°N. All data are used after the linear trend has been removed.

[11] The Linear Baroclinic Model (LBM) developed by *Watanabe and Kimoto* [2000, 2001] is used to reproduce the observed steady atmospheric responses to given SST. This linearized GCM is a spectral model with a triangular truncation at wave number 21 and has 20 vertical levels. In the moist LBM, calculated energy sources associated with cumulus convection are based on a relaxed convective adjustment proposed by *Betts* [1986] and *Betts and Miller* [1986], further referring to a linearization by *Neelin and Yu* [1994]. Sensible and latent heat release at the surface are provided by the respective linearized form of the bulk formula. Details on the LBM are given in Appendix A. Steady SST forcing is prescribed in all experiments in this study. As the atmospheric response was going to be equilibrated after day 10, we examined the response on days 10 through 15 in the LBM experiments.

3. Observational Analysis

[12] To investigate a dynamical process on the modulation of the Walker Circulation associated with El Niño, we chose the 5 biggest El Niño events for which the NINO3.4 SST is larger than 1.2 standard deviations for the composite analysis. The chosen events are 1965/1966, 1972/1973, 1982/1983, 1991/1992, 1997/1998 El Niño events. As shown in Figure 1, the SST is almost uniform from the western to central Pacific. In detail, the maximum location of SST is still over the western Pacific. However, the upward motion is maximized over the central Pacific. This implies that the zonal redistribution of SST during the El

Niño events is not the main mechanism for the zonal displacement of the convection center, and some other dynamical processes are involved in the convection changes.

[13] As well as the reanalysis data, the TRMM satellite data shows a similar feature. Figure 2 shows the January TRMM precipitation over the Pacific basin averaged from 1998 to 2003 (Figure 2a) and 1998 (Figure 2b). Because of the short historical data, we regard the precipitation averaged for 1998–2003 as a climatology. For the climatological precipitation, the maximum precipitation is located over the western Pacific. In this case, the precipitation is likely to be associated with high SST from the western to central Pacific. It seems that zonal distribution of precipitation is proportional to that of SST in climatology. However, the precipitation during January 1998 (Figure 2b) shows different features from climatological precipitation. As well known, the 1997/1998 El Niño was one of the biggest El Niño events of the 20th century. During January 1998, the magnitude of precipitation over the central Pacific was at a maximum (about 10 mm/d). However, as shown in Figure 1, the maximum SST is not collocated with the maximum precipitation during the El Niño events.

[14] The longitudinal difference of convection during the El Niño can be explained by wind vector. Figure 3 shows a perturbation of an 850 hPa wind during the El Niño mature phase. The perturbation is defined as a deviation from the zonal mean. During the El Niño mature phase, similar wind responses like Gill-type solutions are induced over the Pacific region. According to *Gill* [1980], atmospheric heating (precipitation) induces Rossby wave responses over the western part of the forcing and Kelvin wave responses over the eastern part of the forcing. Similarly, easterly winds blow over the eastern Pacific which is associated with Kelvin wave responses. Over the western-central Pacific, cyclonic flows associated with Rossby wave responses are dominant. Note that the signs of the meridional winds over the western and central Pacific are opposite to each other. Over the western Pacific, northerlies (southerlies) are dominant over the Northern (Southern) Hemisphere. On the other hand, over the central Pacific, southerlies (northerlies) are dominant over the Northern (Southern) Hemisphere. Meanwhile, the meridional gradient of moist energy is equatorward and its magnitudes are nearly the same over the whole tropical Pacific basin (not shown). This implies the spatial patterns and signs of meridional moist energy advection are mostly determined by the meridional winds.

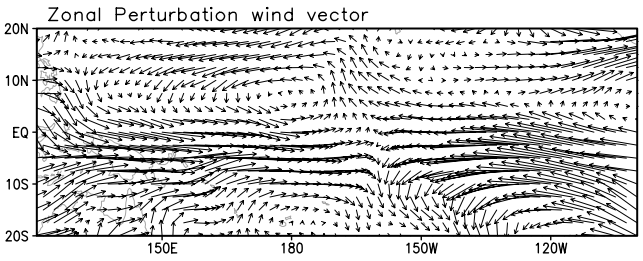

Figure 3. Zonal mean perturbation of 850 hPa wind vector during El Niño mature (DJF) phase.

[15] Therefore cold and dry meridional advection would be induced over the western Pacific through transporting cold and dry moist energy from off the equator to the equator. Over the central Pacific where southerlies (northerlies) over the Northern (Southern) Hemisphere are dominant, warm and wet moist energy advection would be induced. Note that moist energy advection (in a zonal, vertical direction) or diffusion processes should be induced and compensate meridional moist energy when the steady state is assumed. If the vertical moist energy advection is dominant among them, the opposite sign of meridional moist energy advection can cause the opposite tendency in vertical motions between the western to central Pacific.

[16] To investigate the role of moist energy advection quantitatively, we analyze the moist energy budget. Many researchers have used a moist static energy equation to investigate atmospheric behavior over the equatorial region. In particular, some studies have focused on the role of the meridional moist static energy advection on convective activities over the Indo-Pacific sector [*Su and Neelin*, 2002; *Chou*, 2004; *Jiang and Li*, 2005]. In particular, *Chou* [2004] argued that the suppressed convection, which is associated with anomalous low-level anticyclone over the western North Pacific during the El Niño, is mainly induced by a cooling tendency associated with the vertical average of the meridional advection of moist static energy. In the similar manner, we will show here, that moist energy advection play a crucial role in modulating Walker circulation associated with El Niño.

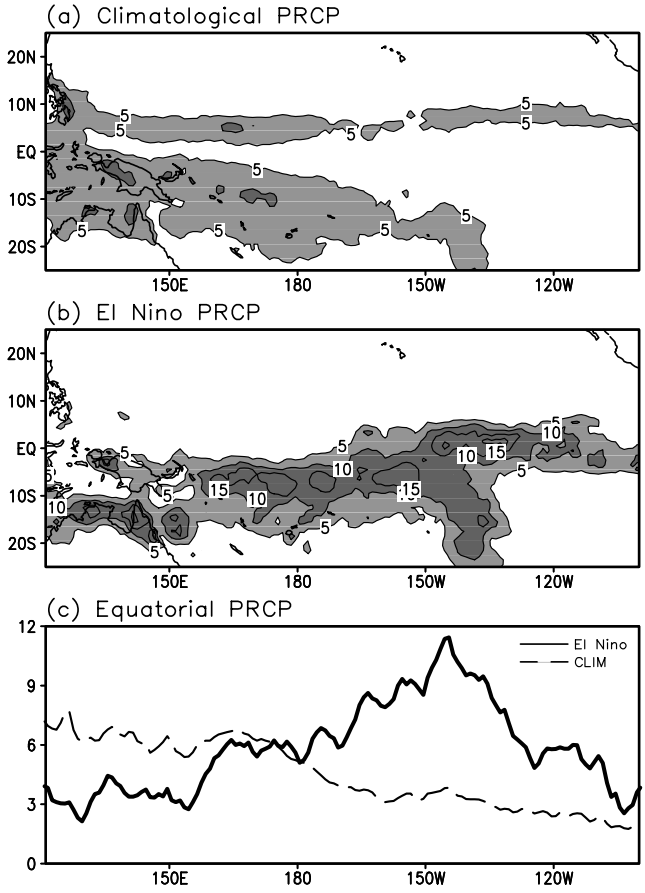

Figure 2. TRMM precipitation during (a) January 1998–2003 and (b) January 1998. (c) Equatorial PRCP averaged between 10°S–10°N. The unit of precipitation is mm/d.

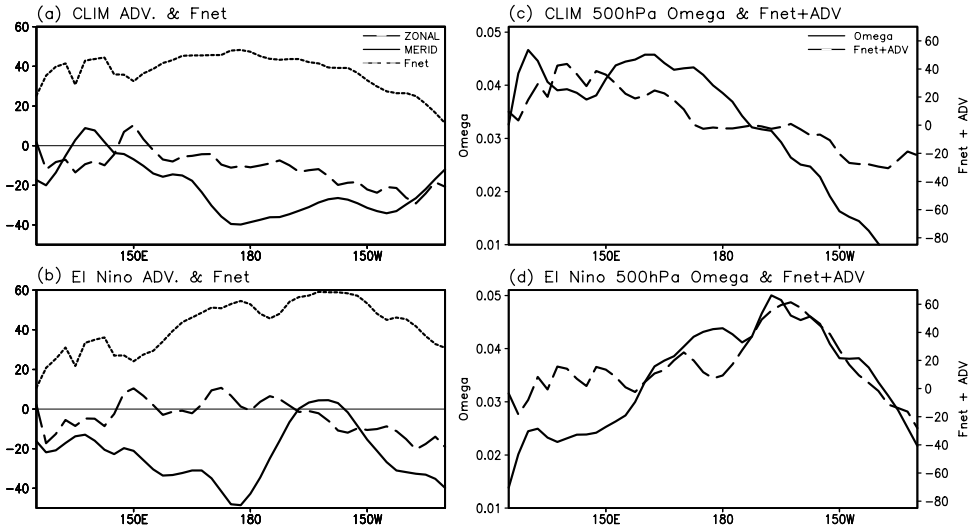

Figure 4. Zonal (dashed line), meridional (solid line) moist energy advection, and net heat flux (dotted line) during (a) DJF climatology and (b) DJF El Niño. (c and d) The 500 hPa vertical velocity (solid line) and sum of zonal, meridional moist energy advection, and net heat flux (dashed line). The units of moist energy budget and vertical pressure velocity are W/m^2 and -1 hPa/s, respectively.

[17] The simplified moist energy equation used in this study is the same as that used by *Neelin and Held* [1987], except that the effect of the horizontal gradient of moist energy is included.

$$w = -\nabla\vec{v}_{low} = \frac{\langle F_{net}\rangle - \frac{1}{g}\int \vec{v}\cdot(\nabla m)dp}{\frac{1}{g}\left(m_{upp} - m_{low}\right)} \qquad (1)$$

where F_{net} means net radiation which includes shortwave radiation, longwave radiation, sensible fluxes and latent heat fluxes into the air column. $\vec{v}$ and m denote wind vector and moist energy, respectively. Moist energy is defined as the sum of temperature, moisture and geopotential height in energy units (e.g., $m = C_pT + Lq + gz$). It should be noted that the magnitude of the vertical gradient of moist energy ($m_{upp} - m_{low}$) is positive and its magnitude is almost same over the Pacific domain (not shown). Then, the simplified equation implies that the vertical motions are only determined by net heat flux and horizontal moist energy advection. For example, upward motion can be generated where there is warm and wet moist energy advection or incoming net radiation. However, note that simple baroclinic structure is assumed to derive the moist energy equation (e.g., one sign in low level, opposite sign in upper level, and small values in the middle troposphere); therefore the equation is valid only over the equatorial regions (within 10°S–10°N).

[18] According to equation (1), vertical motions can be modulated by the moist energy advection and net heat flux. However, the variation of OLR, whose anomalies are largest among the net flux terms during El Niño events, results from the variation in vertical motions. Therefore the equation can be written as $w\propto -\int\vec{v}\cdot(\nabla m)dp$. It means the moist energy advection is a main factor in modulating the vertical motions according to the moist energy equation.

[19] Figure 4 shows the moist energy budget over the equatorial Pacific regions for climatology and El Niño composite during DJF season. For El Niño composite, 1965/1966, 1972/1973, 1982/1983, 1991/1992, 1997/1998 events are used as mentioned before. It is seen that the upward motion is overall consistent with the summation of net heat flux and horizontal advection, though there is local inconsistency over Maritime Continent. In the climatology, the maxima of the upward motion are over the western Pacific. Also, the sum of horizontal moist energy advection and net heat flux is at a maximum over the western Pacific. This spatial distribution is due to the meridional advection, which has large negative values except over the western Pacific. That is, the convection is not favorable because of the meridional cold and dry moist energy advection except over the western Pacific.

[20] During the El Niño mature phase, the meridional advection of moist energy is still important to determine the spatial structure of the Walker Circulation. Note that the magnitude of zonal advection of moist energy and net radiation is almost uniform all over the Pacific domain. It implies that the zonal advection and net radiation cannot determine the spatial pattern of the vertical motions. On the other hand, the meridional advection of moist energy is maximized around the longitudes 160°W. Therefore it creates favorable conditions for upward motion around 160°W during the El Niño mature phase. It is due to the warm and wet moist energy advection in the meridional direction over the central Pacific, which is induced by the southerlies (northerlies) on the Northern (Southern) Hemisphere, as mentioned before. This means the ascending motion, which is associated with adiabatic cooling and cold vertical advection, is generated to compensate for the warming due to warm and wet moist energy advection. On the other hand, the cold and dry moist energy advection over the western Pacific is induced by northerlies (souther-

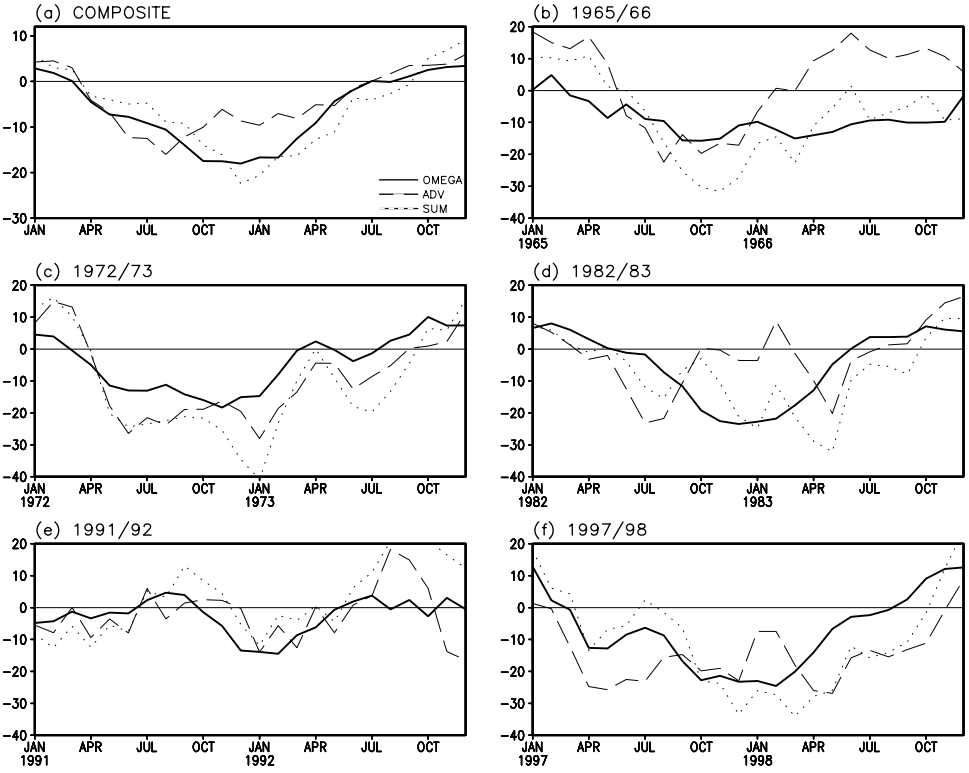

Figure 5. The 500 hPa omega (solid line), sum of zonal, meridional advection of moist energy and net heat flux (dotted line) and meridional advection of moist energy (dashed line) over the western Pacific (120–150°E, 15°S–15°N) during El Niño events. The units of moist energy budget and vertical pressure velocity are W/m^2 and -10^{-4} hPa/s, respectively. Note that the sign of omega is reversed.

lies) on the Northern (Southern) Hemisphere; therefore the descent is generated because of the meridional advection of moist energy.

[21] It is well known that the mean SST distribution is a dominant factor in determining the distribution of convective activity in the tropics. That means, if we consider the effect of SST only, convective activities should be uniform from the western to the central Pacific during the El Niño events. However, a Rossby wave, which arises in response to the convection induced by the uniform SST, can generate the opposite tendency of meridional moist energy advection between the western and central Pacific, which results in the concentration of convective activities over the central Pacific during the El Niño. That is, warm and wet (cold and dry) moist energy advection is induced by the poleward (equatorward) winds on the central (western) Pacific; therefore the ascent (descent) which leads the cold-dry (warm-wet) vertical moist advection is enhanced to balance the horizontal moist energy advection.

[22] Similarly, descent over the western Pacific during El Niño events is due to meridional cold-dry moist energy advection. Figure 5 shows the anomalous moist energy advections, anomalous net heat fluxes and anomalous vertical motions over the western Pacific (120–150°E, 10°S–10°N) during El Niño events. Vertical motions are maximized during the DJF season, because the SST signals associated with the El Niño are also maximized during the DJF season. It is clear that the evolution of the sum of the moist energy budget terms (dotted line) agrees well with that of 500 hPa vertical pressure velocities. This implies that, the simplified moist energy equation is valid to investigate the moist energy budget at the equator. As well as the composite case, the sum of the moist energy budget also agrees well with the vertical motions during each El Niño event. The correlation coefficient between the omega and the sum of moist energy advections and the net heat flux is 0.52 having a 99% significance level. Correlation coefficients between vertical motions and each term of the moist energy equation are summarized in Table 1.

[23] According to Table 1, meridional moist energy advection is mostly well correlated with vertical motions, compared to other terms. The correlation coefficient between meridional advection of moist energy and omega is 0.43, having a 99% significance level. This indicates that the cold and dry moist energy advection induced by the equatorward flow suppresses the convection. Zonal advection of moist energy does not correlate well with vertical motions. In addition, zonal advection of moist energy can be ignored because the magnitude of zonal advection is small (dashed line of Figures 4a and 4b).

[24] The net heat flux term correlates to some degree with vertical motion. It is appeared that Outgoing Longwave Radiation (OLR) is well correlated with vertical motion among the net heat flux terms (e.g., correlation coefficient between OLR and vertical motion is 0.82). The high correlation is due to the fact that the enhanced (suppressed) convective activities raise (lower) the cloud top; therefore it tends to reduce (increase) the OLR. This implies that the

Table 1. Correlation Between 500 hPa Omega and Zonal Advection of Moist Energy, Meridional Advection of Moist Energy, Net Heat Flux, and Sum of Three Terms

	Correlation With Omega
Zonal advection	−0.17
Meridional advection	0.43
Net heat flux	0.29
SUM of three terms	0.52

enhanced OLR does not cause the descent over the western Pacific during El Niño events.

4. Linearized Baroclinic Model (LBM) Experiments

[25] We showed using observational data that the meridional advection of moist energy is critical to the formulation of the anomalous Walker Circulation associated with El Niño. To support our hypothesis, numerical experiments were performed using a Linear Baroclinic Model (LBM) developed by *Watanabe and Kimoto* [2000, 2001].

[26] The LBM has been used to examine the steady atmospheric response to SST forcing in many studies. For example, *Watanabe and Jin* [2003] showed that the present LBM can simulate a realistic atmospheric circulation in response to given SST forcing. Also, *Annamalai et al.* [2005a] showed that model results using the LBM confirm their AGCM's results concerning the impact of Indian Ocean SST anomalies on the developing El Niño. Since the LBM contains most of the physical and dynamical processes that we are stressing here on the modulation of the Walker circulation, the LBM is an appropriate tool to test out our hypothesis.

[27] However, before using the present simplified model, it should be noted that the LBM has some limitations to simulate climate variability exactly. First, nonlinear advection terms cannot be considered in the linear model. Second, air-sea and air-land coupling process is neglected in the LBM. Third, the steady solution is dependent of several parameters in some extent. For example, the magnitude of solution is largely controlled by the damping timescale or an adjustment timescale which determines how fast the temperature and moisture field adjust to reference profile.

[28] To confirm that the LBM is an appropriate tool in this study, in spite of these deficiencies, we investigated the convection responses to the observed zonal mean perturbed SST of the 5 largest El Niño events. Also, zonally averaged DJF climatological values are prescribed as basic states. Since the present LBM is designed to be linearized about zonal mean values, the simulated steady solutions are zonal mean perturbed values. Figure 6 shows the observed and simulated vertical pressure velocity at 500 hPa. Note that zonal mean values are subtracted in observations (Figure 6a) to compare them with simulated ones.

[29] Though magnitudes of vertical motions in the LBM simulation are somewhat stronger than the observed, it is clear that the overall features of the simulated vertical motions are similar to the observed ones. The strong ascending motions are located over the central Pacific both in the observations and the LBM simulations. It implies that the model captures the dominant features of observed convection change during El Niño events. Therefore the model is an appropriate tool to investigate what is the key mechanism in formulating the anomalous Walker Circulation.

[30] However, it is hard to argue that meridional moist energy advection plays an important role in omega response in this experiment: because zonal displacement of the convection center in this experiment can result from many dynamic terms. In addition, the spatial shape and different magnitude of SST forcing can affect the model solutions. Therefore simplified experiments are performed to investigate the role of meridional moist energy advection more clearly. By prescribing simplified basic states and SST forcing, we tried to investigate the role of meridional moist energy advection, as mentioned in the observational analysis.

[31] In control run (CNTL), zonally uniform basic states for atmospheric temperature, moisture and SST are prescribed by taking the zonal mean from the DJF climatological value of the NCEP data. Note that the basic state is also set to be symmetric about the equator. The simplified basic states for the flow and surface pressure are set to zero and 1000 hPa, respectively. A constant bell-type SST forcing is imposed over the equatorial region (150°E–155°W, 10°S–10°N).

[32] To investigate which part of SST is responsible for determining the spatial pattern of convection, we performed additional experiments by separating SST forcing. The "WEST_Forcing" ("EAST_Forcing") experiment indicates that the western half (eastern half) of SST forcing in the CNTL only is given. The same basic states as the CNTL are prescribed. Details of the model experiments are shown in Table 2. It should be noted that the sum of atmospheric responses in "EAST_Forcing" and "WEST_Forcing" runs are equal to that in the control run because the LBM is a linear system on the constant basic state.

[33] Figure 7 shows the 850 hPa wind vector, 500 hPa and equatorial omega in the CNTL, "WEST_Forcing" and "EAST_Forcing." In the CNTL, it is clear that the convec-

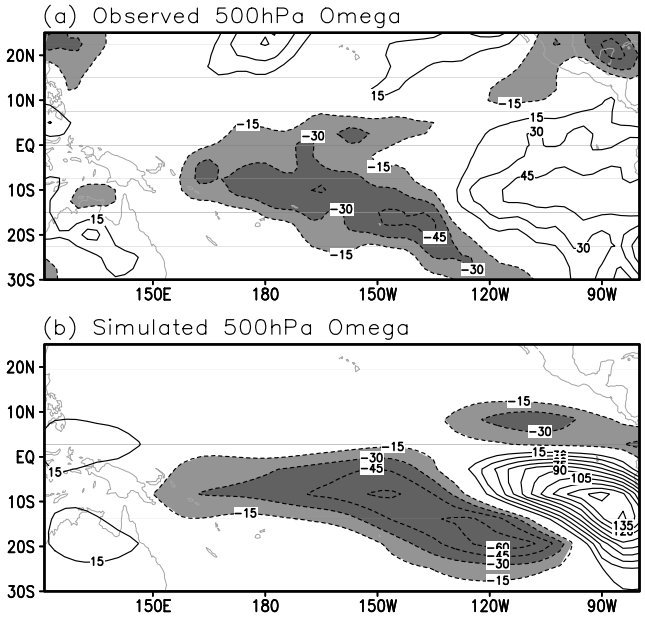

Figure 6. (a) Observed zonal perturbation 500 hPa omega. (b) Simulated 500 hPa omega responses. Zonally averaged and observed basic states are prescribed.

Table 2. Prescribed SST Forcing and Basic States in Idealized Experiments[a]

	SST Forcing			Basic State U	Basic State V	Basic State Pressure	Basic State T and Q
	A + B Forcing	A Forcing	B Forcing				
CNTL	constant Bell-type over 120°E–155°W, 10°S–10°N	western half of "A + B forcing"	eastern half of "A + B forcing"	0 m/s	0 m/s	1000 hPa	zonal mean from 120°E–80°W during DJF season
CON_TQ	constant Bell-type over 120°E–155°W, 10°S–10°N	N/A	N/A	0 m/s	0 m/s	1000 hPa	horizontally constant; vertical profile is still given

[a]N/A, not applicable.

tion maximum is located over the eastern part of SST forcing (thick solid line of Figure 7d). It is consistent with the observation that the convective activities are concentrated over the central Pacific, though the SST is nearly uniform from the western to central Pacific. Also, this is in line with the fact that the magnitude of descent is much stronger to the west of SST forcing than it is to the east of SST forcing. Note that the patterns of atmospheric responses in the "EAST_Forcing" and "WEST_Forcing" basically resemble those in the CNTL, though their zonal scale is different. In addition, the atmospheric responses between the "EAST_Forcing" and "WEST_Forcing" are the same as each other except for some minor differences due to the use of zonally symmetric basic states in the experiments. However, the difference of zonal location of the SST forcing leads to a cancellation between two atmospheric responses. For example, the downward motion in the "EAST_Forcing" around 150°E can cancel the ascent in the "WEST_Forcing" run. On the other hand, the downward motion in "WEST_Forcing" hardly suppress the ascent in "EAST_Forcing." These responses generate the stronger ascent over the eastern part of SST forcing in the CNTL.

[34] Why is the downward motion stronger in the western part of the SST forcing than in the eastern part? In Gill-type solutions, atmospheric Kelvin waves over the east of the forcing induce descending motion over the east of the heating. Also, descending motion associated with Rossby waves appears in the off-equatorial latitudes which are produced by the Sverdrup balance. According to Gill's solution, the magnitude of the descent due to Rossby waves is somewhat stronger than that due to Kelvin waves; however, the difference is not significant. Note that the role of moist energy cannot be considered in the original shallow water equation.

[35] However, when the terms associated with moist energy and its advections are considered, the atmospheric response is different from the traditional one. In CNTL run in this study, the meridional moist energy advection induces the stronger descent over the western part of SST forcing. Figure 8 shows the meridional moist energy advection in a CNTL run. In Figure 8, cold-dry moist energy advection is prominent over the western part of SST forcing. To conserve the moist energy budget, additional descent for the warm-wet vertical moist energy advection and the adiabatic warming is induced. Also, note that the strong descent is concentrated where there is poleward flow. We will compare the atmospheric response with moist energy advection to that without moist energy advection in more detail later.

[36] One more feature of the convection response is that the descent at the western part of forcing is at a maximum in the off-equator region. In addition, the ascent over the eastern edge of SST forcing is latitudinally extended to the off-equatorial region. This is also connected to the spatial structure of meridional advection of moist energy. Note that the meridional advection of moist energy $(-v' \cdot \frac{d\bar{h}}{dy})$ is prominent over the off-equatorial region (Figure 8). The reason is as follows. First, the meridional wind response (v') is stronger in the off-equator region. Second, the basic state meridional gradient of moist energy at the off-equatorial region is larger than that at the equator (not shown). Therefore the cold-dry or warm-wet meridional advection of moist energy is mainly induced over the off-equatorial

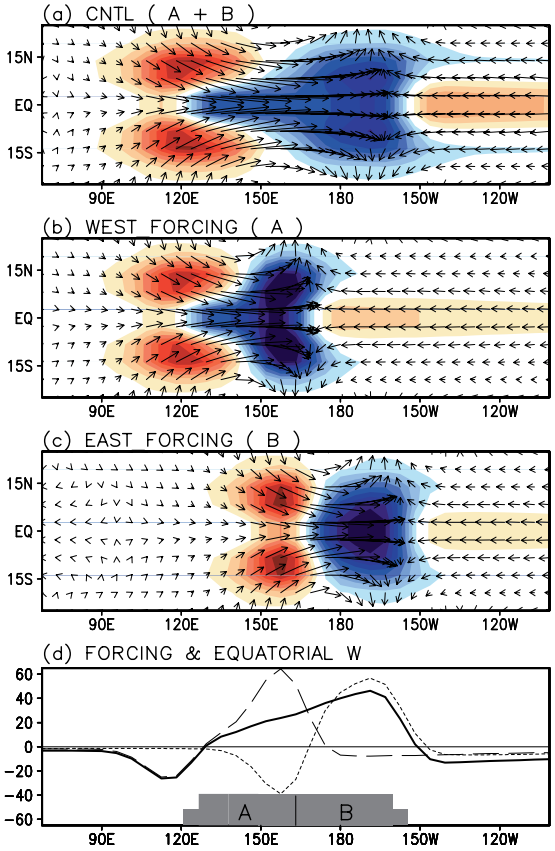

Figure 7. The 500 hPa omega (shading) and 850 hPa wind vector of (a) CNTL run, (b) "WEST_Forcing" run and (c) "EAST_Forcing" run. (d) An equatorial 500 hPa omega of CNTL run (solid line), "WEST_Forcing" run (dashed line) and "EAST_Forcing" run (dotted line). Black shading denotes latitudinally averaged SST forcing. The interval of shading is 10^{-4} hPa/s, and unit of vertical pressure velocity in Figure 7d is -10^{-4} hPa/s.

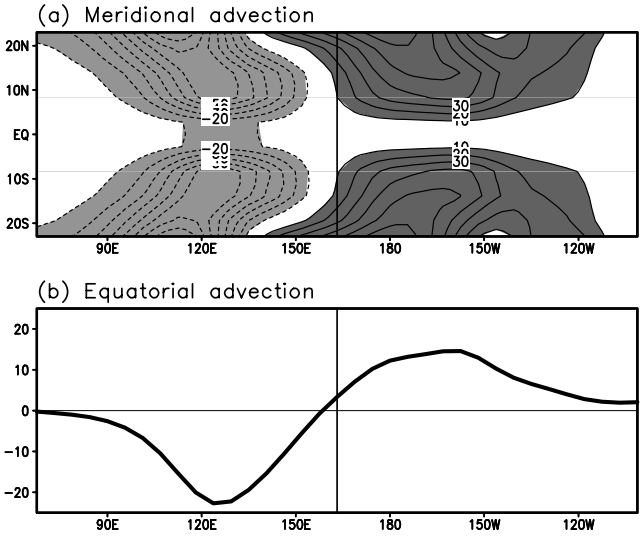

Figure 8. (a) Meridional advection of moist energy in CNTL. (b) Equatorial (15°S–15°N) meridional advection of moist energy. The unit of moist energy advection is W/m^2.

region. It should be noted that the meridional moist energy advection is wholly due to the anomalous wind with equatorward gradients of basic state moist energy.

[37] It has been shown that the meridional advection of moist energy can induce a stronger upward motion over the eastern part of the SST forcing. However, it is questionable whether the meridional advection of the moist energy is enough to explain the zonal asymmetric response of convection to the uniform SST forcing. To prove this, additional experiments are carried out. In the new experiments, the meridional distribution of the temperature and moisture is set to be uniform by prescribing the global mean value. This indicates no horizontal advection of the moist energy. ($-v' \cdot \nabla \overline{h} = 0$). Other conditions are same as for the CNTL. Hereafter, this experiment is known as "CON_TQ" run. Note that the vertical profile of the mean temperature and moisture field is still given.

[38] Figure 9 shows that the 500 hPa omega over the equatorial region (10°S–10°N) in the CNTL and "CON_TQ" runs. In the CNTL, the ascent is maximized over the eastern part of the SST forcing, as mentioned before. Also, the descent over the longitudes 90–120°E is much stronger than that over the longitudes 150–120°W. On the other hand, in "CON_TQ" run, the magnitude of the ascent is nearly uniform, like the pattern of SST forcing. This indicates that meridional moist energy advection plays an important role in the zonal asymmetric responses to the uniform SST forcing. The differences between the two experiments clearly show that the meridional advection of moist energy acts to strengthen (suppress) the convection at the eastern (western) part of SST forcing, as shown in Figure 9c.

[39] Figure 10 shows the 850 hPa stream function and 500 hPa heating field in the CNTL and "CON_TQ" runs. Initially, uniform atmospheric forcing by the given SST induces cyclonic Rossby waves on its west side in the CNTL run. However, as mentioned before, the additional atmospheric heating fields (enhanced convective activities) are generated through the moist energy advection at the eastern edge of cyclones. Note that additional heating is induced by warm-wet moist energy advection due to poleward flows at the eastern edge of cyclones. Because the additional atmospheric forcing forms additional Rossby waves at its west side, the additional cyclones overlap with the original one. Therefore the enhanced heating due to the moist energy advection reinforce the magnitude of original cyclonic Rossby waves. On the other hand, the atmospheric heating over the eastern edge of cyclones cannot be enhanced in the "CON_TQ" run because the meridional moist energy advection is not taken into account. Therefore the magnitude of cyclones in the CNTL run is much stronger (about 3 times) than that it is in the "CON_TQ" run. It implies that low-level cyclonic circulation can modulate the spatial pattern of convective activities through moist energy advection, then, the modulated convections can reinforce the cyclonic Rossby waves again.

[40] In the case of an anticyclone, same mechanism can be applied. When an atmospheric cooling is given, this induces anticyclonic Rossby waves on its west side. Then, the initial cooling is intensified by the local equatorward flows through cold-dry moist energy advection. Because the location of additional atmospheric cooling is the same as that of the initial cooling, the additional anticyclone also overlaps the original one. This means both cyclones and anticyclones are intensified through the meridional moist energy advection, as far as the meridional gradient of moist

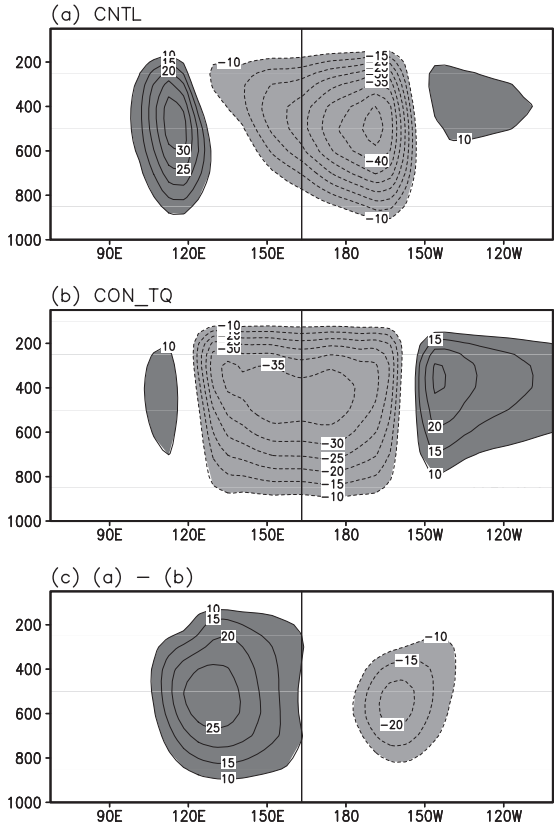

Figure 9. Equatorial (15°S–15°N) omega in (a) CNTL and (b) CON_TQ run. (c) Difference between Figures 9a and 9b. Black (gray) shading denotes downward (upward) motion. The unit of vertical pressure velocity is 10^{-4} hPa/s.

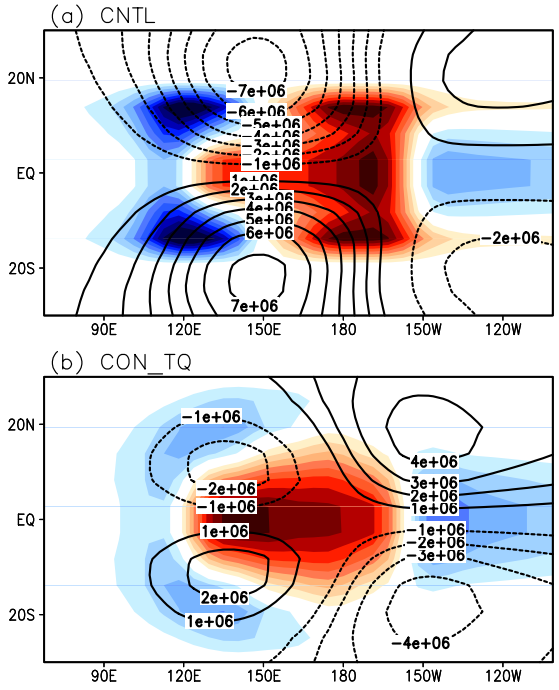

Figure 10. Heating field at 500 hPa (shading) and 850 hPa stream function (contour) at (a) CNTL and (b) CON_TQ run.

energy is poleward. This also implies that the mean meridional gradient of moist energy can be an important factor in determining the magnitude of cyclones or anticyclones, in addition to initial atmospheric heating.

5. Summary and Discussion

[41] During the El Niño mature phase, the warm pool is extended to the central Pacific; therefore the magnitude of SST becomes nearly uniform from the western to central Pacific. However, the maximum convective activity moves from the western to the central Pacific. In this study, dynamical mechanisms of the Walker circulation change during El Niño events are investigated.

[42] The composite analysis and budget analysis with a simplified moist energy equation show that the meridional advection of moist energy plays an important role in the zonal displacement of the convection center during El Niño. Over the western North (South) Pacific, the northerly (southerly) is dominant during the El Niño mature phase. These equatorward winds induce cold-dry moist energy advection over the western Pacific. The cold-dry moist energy advection results in the additional descent over the western Pacific. The idealized experiments using LBM show consistent results with the observational analysis.

[43] Consistent with our study, *Su and Neelin* [2002] emphasized the role of cold and dry air advection on the reduced precipitation associated with El Niño. However, importance of meridional moist energy advection is robust only over the northern descent between the two descending branches over the south and north of the El Niño warm region. This can be explained by hemispheric asymmetry of meridional gradient of moist energy. As well known, the mean meridional gradient of temperature and moisture is stronger over the Northern Hemisphere during the boreal winter time. Then meridional advection of moist energy can overwhelm over the Northern Hemisphere, though the magnitudes of meridional winds over north and south of El Niño warm region are similar to each other. Also, Su and Neelin's results show the insufficient descending motions over the west of El Niño warm region than the observed. They mentioned that this shortcoming may be caused by lack of local SST anomalies. However, lack of meridional moist energy advection due to confined wind anomalies to the east of central Pacific can be another reason for this shortcoming [see *Su and Neelin*, 2002, Figure 2].

[44] As mentioned in introduction, a number of studies have focused on the impact of ENSO on the Indian Ocean. Many of them argued that the Indian Ocean SST variability can modulate the Walker circulation associated with ENSO. Therefore one may argue that zonal displacement of the convection center during the El Niño mature phase results from the effect of warm Indian Ocean SST. To remove the effect of the Indian Ocean SST, the vertical velocity at 500 hPa and SST during El Niño events are investigated when warm Indian Ocean SST anomalies are not detected (e.g., 1965/1966, 1986/1987, 1991/1992, 1994/1995). Zonal displacement of the convection center from the western to the central Pacific is also observed, though warm Indian Ocean SST anomalies are not detected as shown in Figure 11. This indicates downward motion over the western Pacific can be generated without the Indian Ocean SST. However, the magnitude of descending motions over the western Pacific is somewhat weaker without warm Indian Ocean SST anomalies. Therefore one can conclude that Indian Ocean SST anomalies are necessary for capturing the correct intensity of reduced precipitation over the western Pacific, as many studies pointed out [*Annamalai et al.*, 2005a; *Watanabe and Jin*, 2003].

[45] Similarly, there is possibility that other factors which are not dominant in moist energy budget can initiate the descending motions over western Pacific. Because, initiation of reduced convective activities cannot be examined by moist energy budget analysis using data of balanced steady

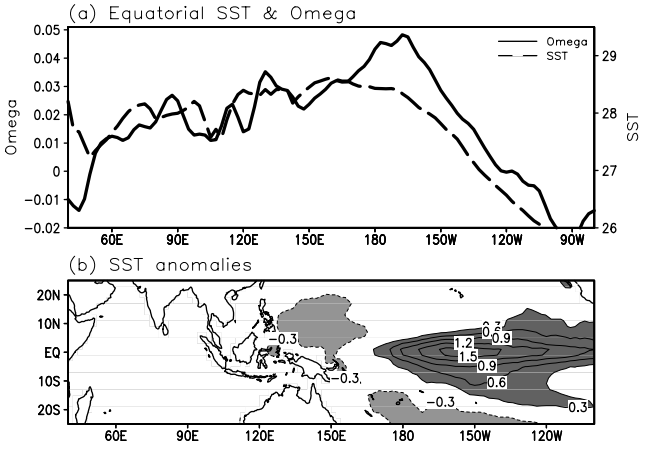

Figure 11. (a) Equatorial 500 hPa omega and total SST and (b) SST anomalies during El Niño events without Indian Ocean Warming.

state (e.g., seasonal mean value during El Niño peak phase). In that case, precise location of descending motion over the western Pacific can be determined by other factors. For example, if nonlinear zonal advection term ($-u'\frac{dT'}{dx}$) is important for initiating the descending motion, then, the initiation of descending motion would be generated over the maximum location of zonal advection term. After that, meridional moist energy advection can play an important role on intensifying the magnitude of reduced convection. Therefore much care should be taken to interpret the results from budget analysis, and, more studies should be examined about the mechanism of determining the precise location of descending motion around the western Pacific in a future.

Appendix A

[46] The linear baroclinic model (LBM) is based on primitive equations used in the CCSR/NIES AGCM. Equations are for vorticity, divergence, logarithm of surface pressure, temperature, and moisture on a vertical sigma coordinate. Because all the primitive equations in LBM are exactly linearized about basic states; therefore the basic states for all prognostic variables of all grid points should be prescribed.

[47] To obtain the heat and moisture sources which should be prescribed in temperature and moisture equations, cumulus convection are also linearly parameterized. The linearized cumulus convection schemes are represented as

$$Q'_c = \frac{e_c}{\tau_c}\left(T'_c - T' - \Delta T'_c\right)$$
$$Q'_q = \frac{e_c}{\tau_c}\left(q'_c - q'\right)$$

[48] Q'_c and Q'_q denote the temperature and moisture source/sink due to cumulus convection. It means that temperature and specific humidity perturbations are restored to reference profiles T'_c, q'_c with an adjustment time τ_c. $\Delta T'_c$ perturbations denotes a temperature correction term to conserve the enthalpy.

[49] Biharmonic horizontal diffusion is applied and e-folding decay time is set to 6 hours. The damping timescale for ζ, D, T is set at 5 d for the lowest two levels and the topmost two levels, and 15 d for the third levels, and 30 d elsewhere. Vertical diffusion, which is set at $(1000\ \mathrm{d})^{-1}$, is also included in order to suppress a vertical computational mode. Large-scale condensation process is not applied. Also, we did not consider the effect of soil wetness (e.g., fixed as constant).

[50] **Acknowledgments.** This work is supported by the Korea Meteorological Administration Research and Development Program under grant CATER_2007-4206 and the second stage of the Brain Korea 21 Project.

References

Annamalai, H., S. P. Xie, and J. P. McCreary (2005a), Impact of Indian Ocean sea surface temperature on developing El Niño, *J. Clim.*, *18*, 302–319.

Annamalai, H., L. Ping, and S. P. Xie (2005b), Southwest Indian Ocean SST variability: Its local effect and remote influence on Asian monsoons, *J. Clim.*, *18*, 4150–4166.

Annamalai, H., K. Hamilton, and K. R. Sperber (2007), The south Asia summer monsoon and its relationship with ENSO in the IPCC AR4 simulations, *J. Clim.*, *20*, 1071–1092.

Betts, A. K. (1986), A new convective adjustment scheme. Part I: Observational and theoretical basis, *Q. J. R. Meteorol. Soc.*, *112*, 677–691.

Betts, A. K., and M. J. Miller (1986), A new convective adjustment scheme. Part II: Single column tests using GATE wave, BOMEX, ATEX and arctic air-mass data sets, *Q. J. R. Meteorol. Soc.*, *112*, 693–709.

Chou, C. (2004), Establishment of the low-level wind anomalies over the western North Pacific during ENSO development, *J. Clim.*, *17*, 2195–2212.

Jiang, X., and T. Li (2005), Reinitiation of the boreal summer intraseasonal oscillation in the tropical Indian Ocean, *J. Clim.*, *18*, 3777–3795.

Gill, A. E. (1980), Some simple solutions for heat-induced tropical circulation, *Q. J. R. Meteorol. Soc.*, *106*, 447–462.

Kalnay, E., et al. (1996), The NCEP/NCAR 40-year reanalysis project, *Bull. Am. Meteorol. Soc.*, *77*, 437–471.

Kang, I.-S., et al. (2002), Intercomparison of GCM simulated anomalies associated with the 1997–98 El Niño, *J. Clim.*, *15*, 2791–2805.

Kidson, J. W. (1975), Tropical eigenvector analysis and the Southern Oscillation, *Mon. Weather Rev.*, *103*, 187–196.

Kug, J.-S., and I.-S. Kang (2006), Interactive feedback between ENSO and the Indian Ocean, *J. Clim.*, *19*, 1784–1801.

Kug, J.-S., T. Li, S.-I. An, I.-S. Kang, J.-J. Luo, S. Masson, and T. Yamagata (2006a), Role of the ENSO–Indian Ocean coupling on ENSO variability in a coupled GCM, *Geophys. Res. Lett.*, *33*, L09710, doi:10.1029/2005GL024916.

Kug, J.-S., B. P. Kirtman, and I.-S. Kang (2006b), Interactive feedback between ENSO and the Indian Ocean in an interactive ensemble coupled model, *J. Clim.*, *19*, 6371–6381.

Lau, N.-C., and M. J. Nath (2003), Atmosphere-ocean variations in the Indo-Pacific sector during ENSO episodes, *J. Clim.*, *16*, 3–20.

Neelin, J. D., and I. M. Held (1987), Modeling tropical convergence based on the moist static energy budget, *Mon. Weather Rev.*, *115*, 3–12.

Neelin, J. D., and J.-Y. Yu (1994), Modes of tropical variability under convective adjustment and the Madden-Julian oscillation. Part I: Analytical theory, *J. Atmos. Sci.*, *51*, 1876–1894.

Reynolds, R. W. (1988), A real-time global sea surface temperature analysis, *J. Clim.*, *1*, 75–86.

Reynolds, R. W., and T. M. Smith (1994), Improved global sea surface temperature analyses using optimum interpolation, *J. Clim.*, *7*, 929–948.

Saravanan, R., and P. Chang (2000), Interactions between tropical Atlantic variability and El Niño–Southern Oscillation, *J. Clim.*, *13*, 2177–2194.

Su, H., and J. D. Neelin (2002), Teleconnection mechanisms for tropical Pacific descent anomalies during El Niño, *J. Atmos. Sci.*, *59*, 2694–2712.

Wang, C. (2000), On the atmospheric responses to tropical Pacific heating during the mature phase of El Niño, *J. Atmos. Sci.*, *57*, 3767–3781.

Watanabe, M., and F.-F. Jin (2003), A moist linear baroclinic model: Coupled dynamical-convective response to El Niño, *J. Clim.*, *16*, 1121–1139.

Watanabe, M., and M. Kimoto (2000), Atmosphere-ocean thermal coupling in the North Atlantic: A positive feedback, *Q. J. R. Meteorol. Soc.*, *126*, 3343–3369.

Watanabe, M., and M. Kimoto (2001), Corrigendum, *Q. J. R. Meteorol. Soc.*, *127*, 733–734.

Wu, R., and B. Wang (2000), Interannual variability of summer monsoon onset over the western North Pacific and the underlying processes, *J. Clim.*, *13*, 2483–2501.

Xie, P., and P. A. Arkin (1997), Global precipitation: A 17-year monthly analysis based on gauge observations, satellite estimates, and numerical model outputs, *Bull. Am. Meteorol. Soc.*, *787*, 2539–2558.

Y.-G. Ham and I.-S. Kang, School of Earth and Environment Sciences, Seoul National University, Seoul 151-742, South Korea. (kang@climate.snu.ac.kr)

J.-S. Kug, Climate Environment System Research Center, Seoul National University, Seoul 151-742, South Korea. (jskug@climate.snu.ac.kr)